OPEN ACCESS
JOURNAL OF ADVANCED DIELECTRICS
Vol. 13, No. 5 (2023) 2350017 (6 pages)

DOI: 10.1142/S2010135X23500170

Effect of grain size on ferroelectric and dielectric properties of $Bi_{3.25}La_{0.75}Ti_3O_{12}$ thin films prepared by rf-magnetron sputtering

Shuai Ma[*,†,¶], Wei Li[‡], Jigong Hao[‡], Yuying Chen[*] and Zhijun Xu[§]

[*]*School of Medicine, Liaocheng University, Liaocheng 252059, P. R. China*

[†]*Beijing Key Laboratory of Digital Stomatology, Beijing 100081, P. R. China*

[‡]*School of Materials Science and Engineering, Liaocheng University Liaocheng 252059, P. R. China*

[§]*School of Environment and Materials Engineering, Yantai University Yantai 264005, P. R. China*

[¶]mashuai@lcu.edu.cn

Received 25 June 2023; Revised 19 July 2023; Accepted 23 July 2023; Published 7 August 2023

$Bi_{3.25}La_{0.75}Ti_3O_{12}$ (BLT) thin films are promising materials used in non-volatile memories. In this work, BLT films were deposited on Pt(111)/Ti/SiO_2/Si substrates by rf-magnetron sputtering method followed by annealing treatments. The microstructures of BLT thin films were investigated via X-ray diffraction (XRD), scanning electron microscopy (SEM) and atomic force microscopy (AFM). With the increase in annealing temperature, the grain size increased significantly and the preferred crystalline orientation changed. A well-saturated hysteresis loop with a superior remnant polarization of 15.4 $\mu C/cm^2$ was obtained for BLT thin films annealed at 700°C. The results show that the dielectric constant decreased with the increase in grain sizes.

Keywords: Thin films; rf-magnetron sputtering; ferroelectric properties; dielectric properties.

1. Introduction

Ferroelectric thin films have been extensively studied for a wide range of applications, such as microsensor arrays, memories, radio-frequency devices, energy storages, photocatalysts, etc.[1–6] Among the ferroelectric thin films, bismuth layer-structured ferroelectrics (BLSFs) are useful lead-free materials due to their superior ferroelectric properties. $Bi_4Ti_3O_{12}$ is a typical BLSF material with three layers, which consists of bismuth oxide layers $(Bi_2O_3)^{2+}$ and perovskite-like layers $(A_{n-1}B_nO_{3n+1})^{2-}$ along the *c*-axis.[7,8] Lanthanum-doped bismuth titanate thin films, reported as $La_{0.75}Bi_{3.25}Ti_3O_{12}$ (BLT), have driven a great interest in non-volatile ferroelectric applications mainly owing to their high fatigue endurance limit.[9] Structurally, BLT consists of triple layers of Ti–O octahedral between $(Bi_2O_3)^{2+}$ layers, where La substitutes for Bi atoms only in the perovskite-type unit.[10] In the last years, dielectric capacitors have been a kind of special energy storage device due to their high power densities and ultrafast charge/discharge rates.[11] It is found that BLT/$SrTiO_3$ multilayer films exhibited excellent energy storage performance.[12] BLT ferroelectric thin films have been fabricated by numerous techniques, such as pulsed laser deposition (PLD), sol–gel method, and rf-magnetron sputtering.[13–15] Rf-magnetron sputtering technique shows advantages in industrial applications as fabricating films with larger areas and better uniformity. In our previous studies, we found the ceramics target's utilization rate was not high, because the sputtering gas argon emits a strong light blue glow during magnetron sputtering, forming a halo and the halo's target is the most serious part bombarded by ions. Based on an overall consideration, we chose the rf-magnetron sputtering route to prepare BLT thin films with different grain sizes in this paper. The microstructures, ferroelectric properties, and dielectric properties of BLT thin films have been investigated.

2. Experimental

BLT thin films were fabricated by a rf-magnetron sputtering method on Pt(111)/Ti/SiO_2/Si substrate. $Bi_{3.25}La_{0.75}Ti_3O_{12}$+ 30mol.% Bi_2O_3 ceramic was used as a target, which can compensate for bismuth element loss caused by bismuth volatilization during sputtering. The target, suitable for rf-magnetron sputtering experiments, was prepared by a hot press sintering. The BLT powder was mixture of Bi_2O_3 (99.99%, Macklin, China), La_2O_3 (99.99%, Macklin, China) and TiO_2 (99.99%, Macklin, China). The powders were embedded in a

[¶]Corresponding author.

carbon die and sintered at 800°C with a pressure of 20MP. It is worth noting that the sintered ceramic was then heat-treated at 800°C for 30 min in air to remove the impurity. Because the ceramic sintered in the carbon die was dark gray due to the diffusion of carbon element. After that, the ceramic target was located about 40 mm from the substrate in the chamber. The deposition was performed at room temperature in pure Ar gas flow. The working pressure was kept at 0.7 Pa and the rf-power was fixed at 50 W. All BLT thin films were deposited for 1h with the same deposition parameters. Then, the as-deposited thin films were annealed ranging from 600°C to 700°C in air for 60min by a special heat process. To fabricate a capacitor structure, an array of circular Au top electrodes was patterned using the thermal evaporation method with a shadow mask.

The crystallization of thin films was performed by X-ray diffraction (XRD; Bruker D8 Advance, Karlsruhe, Germany). The microstructures and elemental composition of BLT thin films were detected by atom force microscopy (AFM; Icon, Burker Corporation, Santa Barbara, US) and a scanning electron microscopy (SEM; Quanta FEG 250, FEI, Hillsboro, OR, USA). Ferroelectric and dielectric properties were measured by a ferroelectric analyzer (TF-2000, aix-ACCT, Aachen, Germany) and a capacitance meter (Agilent 4294A, Agilent Inc., American).

3. Results and Discussions

Figure 1 shows the XRD patterns of BLT thin films annealed at 600°C and 700°C, respectively. The characteristic (111) peak for platinum of the substrates is observed in 2θ ranging between 37° and 45°. All the annealed BLT thin films exhibit similar diffraction peaks, corresponding with the standard diffraction pattern of Aurivillius $Bi_4Ti_3O_{12}$ phase (JCPDS 73-2128, a=0.541 nm, b=0.5448 nm, and c=3.284 nm). However, comparing the XRD data of the two samples,

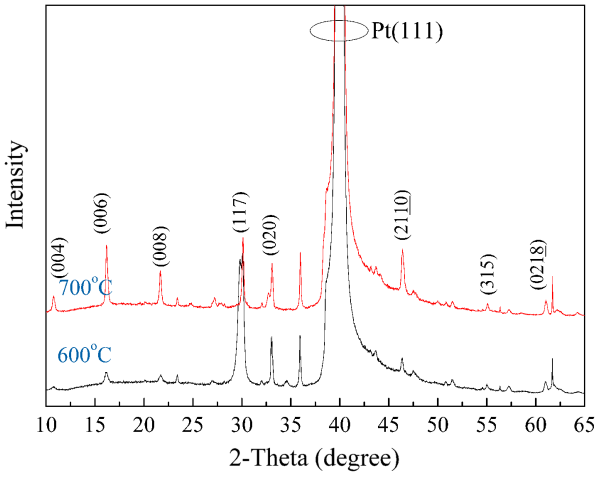

Fig. 1. XRD patterns of BLT thin films annealed at 600°C and 700°C.

it is found that the relative intensities of the diffraction peaks of different crystal planes are obviously different. In view of orientation-sensitive ferroelectric properties in bismuth titanate-based materials, the proportion of (117)-oriented grains was estimated. Simplified approximation of the 117-orientation degree (α) was evaluated according to $\alpha=I_{117}/(I_{117}+I_{006})$, where I_{006} and I_{117} were the intensities of X-ray diffraction peaks for (006) and (117), respectively.[16] An offset process was used in the XRD patterns to reduce the measuring error. The calculated α was 0.88 for thin film annealed at 600°C and increased to 0.52 for thin film annealed at 700°C. This result indicates that with the increase of annealing temperature, the preferred crystalline orientation was changed. When annealed at 600°C, the BLT film was oriented in the ⟨117⟩ direction preferentially. With the annealing temperature increased to 700°C, the film was oriented in a mixed orientation of the c-axis and the ⟨117⟩ direction. As in $Bi_4Ti_3O_{12}$ thick films, the preferred orientation is attributed to the anisotropic shrinkage and morphological changes in particles during heating.[17] Similar mechanism might be occurred in this study.

Figures 2(a) and 2(b) show the surfaces and corresponding cross-sections of BLT thin films annealed at 600°C and 700°C, while their AFM images are displayed in Figs. 2(c) and 2(d), respectively. The dense and plate-like shaped grain formation is observed in both 600°C and 700°C BLT thin films. The formation of plate-like grains is attributed to the anisotropic growth of $Bi_4Ti_3O_{12}$-based materials. The cross-section images reveal that thickness values are similar, which are 670 nm and 600 nm for 600°C and 700°C samples, respectively. The grain size increased significantly with the increase in annealing temperature. In addition, Figs. 2(c) and 2(d) reveal that the grain size directly influenced the surface roughness of the films. The surface roughness of the 700°C annealed thin film was much higher than that of 600°C annealed thin film, which was 24.4 nm for the former and 8.3 nm for the latter.

To analyze the element distribution in grains and grain boundaries, an energy dispersive spectrometer (EDS) as well as element line scanning of 700°C BLT thin films had been performed and the results are shown in Fig. 3. In the EDS image, La characteristic peaks are negligible, due to the small amounts of La element doped in BLT. During the element line scanning measurement, the scanning line crossed several grains. As shown in the image, the peak intensities of Bi, O, Ti and La almost remain unchanged, indicating that all the elements in BLT thin films had a uniform distribution, regardless of their location in grains or grain boundaries.

Ferroelectric polarization–electric field (P–E) hysteresis loops BLT thin films annealed 600°C and 700°C measured at room temperature with a frequency of 1 KHz are displayed in Fig. 4(a). BLT thin film annealed at 700°C reveals a well-saturated hysteresis loop with a remnant polarization ($2P_r$) of 16.8 μC/cm^2 and a coercive electric field ($2E_c$) of 216 kV/cm. This result is similar with those of BLT thin films grown by pulsed-laser deposition, whose remanent polarization ($2P_r$)

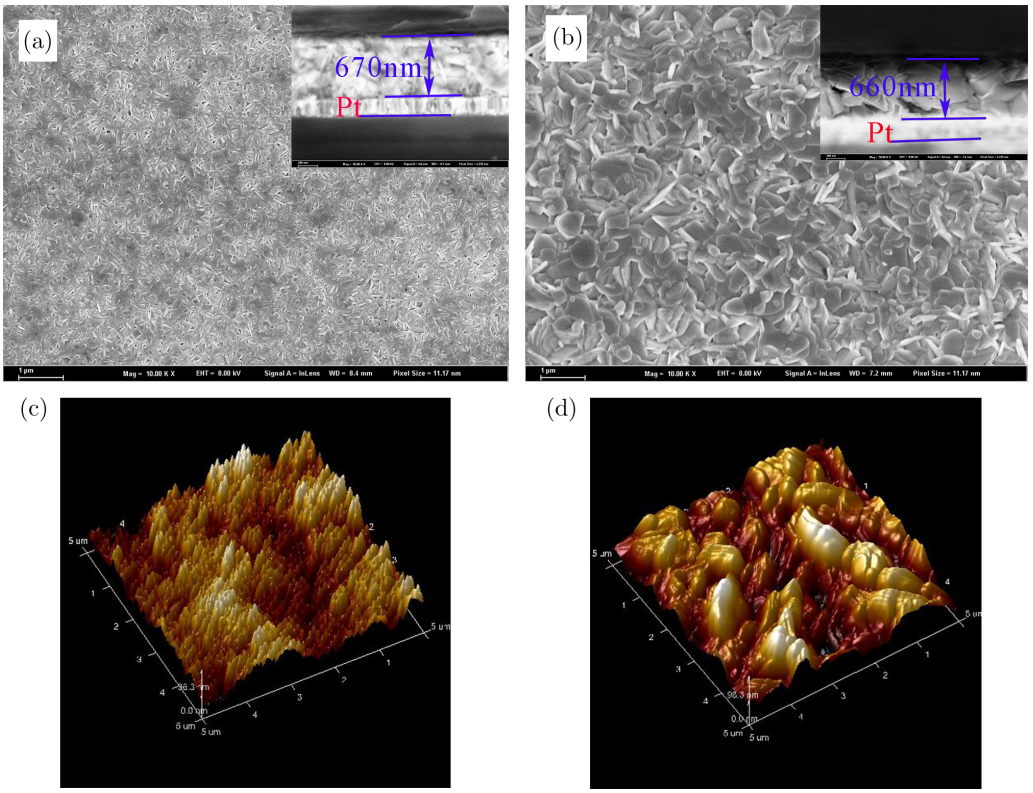

Fig. 2. The surface and cross-section micrographs of BLT thin films: (a) 600°C, (b) 700°C, and AFM images of BLT thin films: (c) 600°C, (d) 700°C.

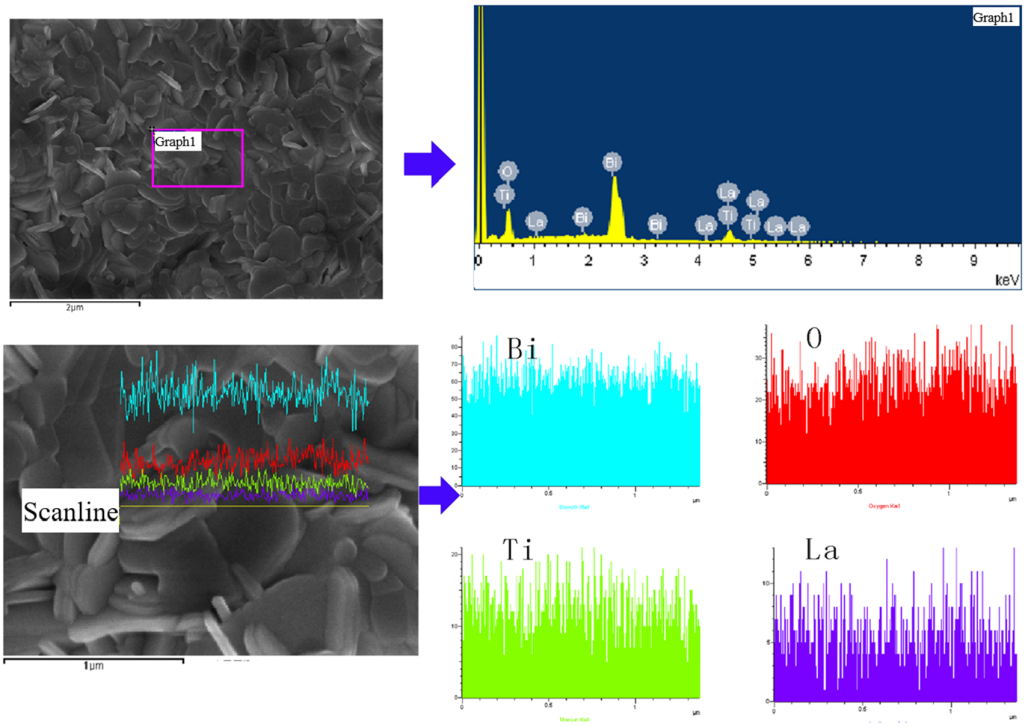

Fig. 3. EDS and element line scanning results of BLT thin film annealed at 700°C.

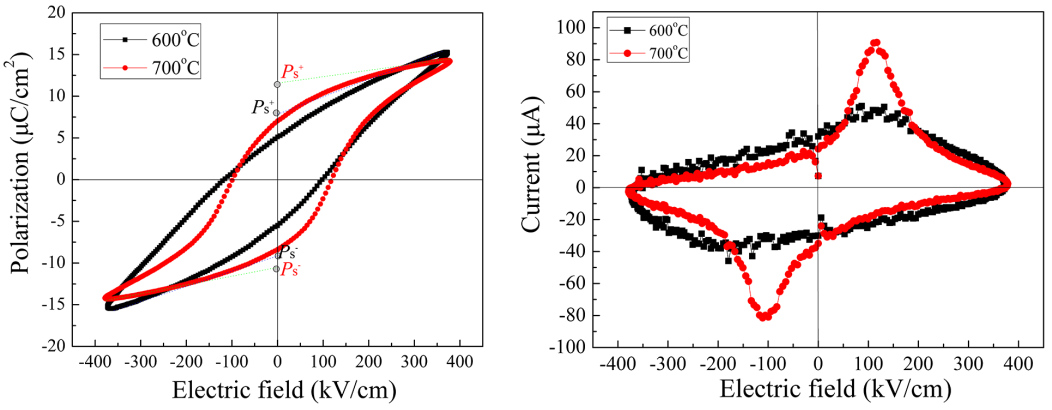

Fig. 4. *P–E* hysteresis loops and *I–E* curves recorded during the *P–E* curve measurement of BLT thin films annealed at 600°C and 700°C: (a) *P–E* hysteresis loops; (b) *I–E* curves.

and coercive field ($2E_c$) were 16 μC/cm^2 and 168 kV/cm.[18] Note that the coercive electric field of the 600°C annealed sample had almost the same value, which was 215 kV/cm, but the remnant polarization ($2P_r$) was much lower than that of the 700°C annealed sample, which was 10.6 μC/cm^2. Moreover, its max polarization under an applied electric field around 400 kV/cm was slightly lower than those of 600°C annealed thin film, but the calculated spontaneous polarization ($2P_s$) was much higher (23.8 μC/cm^2) than the latter (17.4 μC/cm^2). Therefore, the ferroelectric properties are improved significantly with the increase in grain sizes. The spontaneous polarization of $Bi_4Ti_3O_{12}$-based ferroelectrics mainly originates from relative displacement between A-site Bi atom and [TiO_6] octahedra within the perovskite-like layers.[19] It is speculated that the enlargement of grain size could increase the ionic displacement in the unit cells, thus enhancing ferroelectric properties. The *I–E* curves recorded during the hysteresis loop measurement are shown in Fig. 4(b). Both samples have current peaks in the positive and negative current regions, but the current peaks of the films annealed at 600°C are wide and diffuse, and the current peaks of the films annealed at 700°C are relatively sharp. All the current peaks are located in the vicinity of the corresponding coercive field, indicating that the current peaks are caused by the ferroelectric domain inversion in the film. Comparing the hysteresis loops of the two samples, it is found that near the coercive field, the steeper the remanent polarization curve, that is, the greater the polarizability, the greater the peak value of the current peak in the *I–V* curve.

Figure 5 shows the fatigue curves of BLT films with different annealing temperatures tested at room temperature. The test frequency was 10 MHz, and the fatigue voltage was 10 V. The BLT film annealed at 600°C shows fatigue-free behavior up to 10^9 switching cycles. The film annealed at 700°C shows small degradation in the course of 10^9 switching cycles. In general, both BLT films had excellent fatigue resistance. It is reported that the polarization fatigue in perovskite

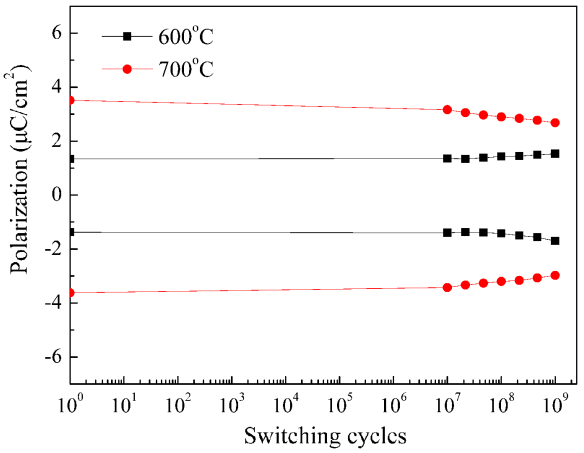

Fig. 5. Polarization fatigue characteristics of BLT thin films annealed at 600°C and 700°C.

ferroelectrics is mainly attributed to the pinning of domain wall motion caused by the oxygen vacancies.[20] Therefore, the film annealed at 700°C might own less oxygen vacancies than the film annealed at 600°C.

The dielectric constants (ε_r) and loss tangents (tan δ) BLT thin films annealed 600°C and 700°C were measured at room temperature as a function of frequency ranging from 1 kHz to 3000 kHz. As shown in Fig. 6(a), the dielectric constants of 600°C BLT at various frequencies are much higher than those of 700°C BLT, e.g., ε_r at 1 kHz is 193 for 600°C BLT and 110 for 700°C BLT, respectively. In addition, the ε_r of 600°C BLT decreased slightly with the increase of frequency, and a similar change law is observed for ε_r of 700°C BLT within frequency region below 110 kHz.

This phenomenon is due to that the electric dipoles are unable to keep pace with the applied electric field in high frequency condition.[21] As the frequency reached above 110 kHz, a sudden decrease is observed in the dielectric constant of 700°C BLT. The decrease in dielectric constant with

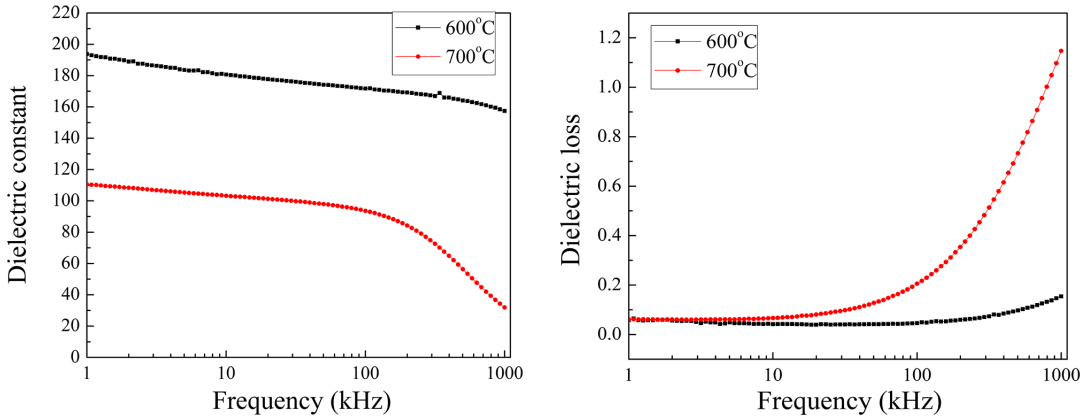

(a) (b)

Fig. 6. Dielectric constants and loss tangents as a function of frequency for BLT thin films annealed at 600°C and 700°C.

increasing frequency might be caused by the extrinsic resonance behavior induced by the charges trapped at interface states that followed the altering current.[22] Frequency dependence of loss tangents of BLT annealed at 600°C and 700°C are plotted in Fig. 6(b). In agreement with the dielectric constant result, the loss tangents of 700°C BLT increased significantly in high-frequency region. The anomalous dispersion at high frequency might be attributed to space charge polarization or Maxwell–Wagner-type interfacial polarization.[23] The measured frequency might be corresponding to the resonant frequency of the thin films annealed at 700°C with the conventional dielectric bridges measurement circuit.

4. Conclusions

BLT thin films with different grain sizes were fabricated on Pt(111)/Ti/SiO_2/Si substrates using the rf-magnetron sputtering method with a deposition atmosphere of Ar. After annealing treatment, both BLT thin films exhibited a dense structure with plate-like grains. XRD patterns and SEM images indicate that thin films were well crystalline and the surface roughness was elevated with the increase of grain sizes. The thin film annealed at 700°C exhibited well-saturated hysteresis loops with a superior remnant polarization of 15.4 μC/cm^2 and a coercive field of 216 kV/cm. In addition, it was found that dielectric constants of 700°C annealed thin films decrease significantly with the increase of grain sizes. In general, the rf-magnetron sputtering process method used in this study could be a promising way to prepare $Bi_4Ti_3O_{12}$-based thin films with excellent ferroelectric properties.

Acknowledgments

This work was supported by the Research Foundation of Liaocheng University (No. 318051939), Opening Project of Beijing Key Laboratory of Digital Stomatology (PKUSS20210301), Natural Science Foundation of Shandong Province of China (Nos. ZR2020ME031, ZR2020ME033), Innovation Team of Higher Educational Science and Technology Program in Shandong Province (No. 2019KJA025).

References

[1]N. Setter *et al*., Ferroelectric thin films: Review of materials, properties, and applications, *J. Appl. Phys.* **100**, 51606 (2006).
[2]Y. Zhao *et al*., Lead-free $Bi_{5-x}La_xTi_3FeO_{15}$ (x=0,1) nanofibers toward wool keratin-based biocompatible piezoelectric nanogenerators, *J. Mater. Chem. C* **4**, 7324 (2016).
[3]L.W. Martin and A. M. Rappe, Thin-film ferroelectric materials and their applications, *Nat. Rev. Mater*. **2**, 16087 (2016).
[4]J.W. Lee *et al*., In-plane quasi-single-domain $BaTiO_3$ via interfacial symmetry engineering, *Nat. Commun*. **12**, 6784 (2021).
[5]S. Ma *et al*., Influence of tantalum on mechanical, ferroelectric and dielectric properties of Bi-excess $Bi_{3.25}La_{0.75}Ti_3O_{12}$ thin film, *Appl. Surf. Sci.* **463,** 1141 (2019).
[6]J. Qian *et al*., High energy storage performance and large electrocaloric response in $Bi_{0.5}Na_{0.5}TiO_3$-$Ba(Zr_{0.2}Ti_{0.8})O_3$ thin films, *ACS Appl. Mater. Interfaces* **14**, 54012 (2022).
[7]C. Long *et al*., Crystal structure and enhanced electromechanical properties of Aurivillius ferroelectric ceramics, Bi_4Ti_{3-x}-$(Mg_{1/3}Nb_{2/3})_xO_{12}$, *Scripta Mater.* **75**, 70 (2014).
[8]A. R. Chaudhuri, A. Laha and S. B. Krupanidhi, Enhanced ferroelectric properties of vanadium doped bismuth titanate (BTV) thin films grown by pulsed laser ablation technique, *Solid State Commun.* **133**, 611 (2005).
[9]B. H. Park *et al*., Lanthanum-substituted bismuth titanate for use in non-volatile memories, *Nature* **401**, 682 (1999).
[10]J. Qian *et al*., Energy storage performance of flexible NKBT/NKBT-ST multilayer film capacitor by interface engineering, *Nano Energy* **74**, 104862 (2020).
[11]W. Yue *et al*., High energy storage density of $Bi_{3.25}La_{0.75}Ti_3O_{12}$/$SrTiO_3$ multilayer thin films by structural design, *Mater. Lett.* **333**, 133576 (2023).
[12]Y. Shimakawa *et al*., Crystal and electronic structures of $Bi_{4-x}La_x$-Ti_3O_{12} ferroelectric materials, *Appl. Phys. Lett.* **79**, 2791 (2001).
[13]M. P. Besland *et al*., Comparison of lanthanum substituted bismuth titanate (BLT) thin films deposited by sputtering and pulsed laser deposition, *Thin Solid Films* **495**, 86 (2006).
[14]W. Aiying *et al*., Sol–gel synthesis and electrical characterization of $Bi_{3.25}La_{0.75}Ti_3O_{12}$ thin films, *Mater. Res. Bull.* **47**, 3819 (2012).

[15]S. Ma *et al*., Characterization of highly (117)-oriented $Bi_{3.25}La_{0.75}Ti_3O_{12}$ thin films prepared by rf-magnetron sputtering technique, *Solid State Commun*. **278**, 31 (2018).
[16]H. N. Lee *et al*., Ferroelectric $Bi_{3.25}La_{0.75}Ti_3O_{12}$ films of uniform *a*-aixs orientation on silicon substrates, *Science* **296**, 2006 (2002).
[17]Y. Kinemuchi *et al*., Preferred orientation of $Bi_4Ti_3O_{12}$ thick film, *J. Am. Ceram. Soc.* **90**, 2753 (2010).
[18]J.H. Park and J. B. Kim, Electric response as a function of applied voltage of $Bi_{3.25}La_{0.75}Ti_3O_{12}$ thin films grown by pulsed-laser deposition, *Mater. Sci. Eng. B* **128**, 250 (2006).
[19]J.A. Bartkowska, J. Dercz and D. Michalik, The origin of the ferroelectricity in the bismuth titanate $Bi_4Ti_3O_{12}$ with perovskite-like layered structure, *Solid State Phenom.* **226**, 17 (2015).
[20]J. F. Scott and M. Dawber, Oxygen-vacancy ordering as a fatigue mechanism in perovskite ferroelectrics, *Appl. Phys. Lett*. **76**, 3801 (2000).
[21]P. Lv *et al*., 4-inch ternary $BiFeO_3$–$BaTiO_3$–$SrTiO_3$ thin film capacitor with high energy storage performance, *ACS Energy Lett*. **6**, 3873 (2021).
[22]A. Marikani *et al*., Ferroelectric, dielectric, and optical properties of Nd-substituted $Bi_4Ti_3O_{12}$ nanoparticles synthesized by sol–gel method, *Prog. Nat. Sci.-Mater*. **26**, 528 (2016).
[23]F. M. Pontes *et al*., Effects of the post annealing atmosphere on the dielectric properties of $(Ba,Sr)TiO_3$ capacitors: Evidence of an interfacial space charge layer, *Appl. Phys. Lett*. **76**, 2433 (2000).